

ORIGINAL RESEARCH

Open Access



Biochar reduces colloidal phosphorus in leachate by regulating *phoD*- and *phoC*-harboring microbial communities during drying/rewetting cycles

Xiaochun Wang¹, Hongnuo Ge², Yuning Fang³, Chunlong Liu⁴, Kamel M. Eltohamy¹, Zekai Wang¹ and Xinqiang Liang^{1,4*}

Abstract

Drying and rewetting (DRW) events cause the release of colloidal phosphorus (P_{coll} , 1–1000 nm) in leachate, and biochar is considered an effective inhibitor; however, the microbial mechanism remains elusive. In this study, three successive DRW cycles were performed on the soil columns to assess the effect of biochar addition on P_{coll} content and its possible associates, including phosphatase-producing microbial populations (*phoD*- and *phoC*-harboring microbial communities) and alkaline/acid phosphatase (ALP/ACP) activities. Results showed that the biochar addition significantly decreased the P_{coll} by 15.5–32.1% during three DRW cycles. The structural equation model (SEM) confirmed that biochar addition increased *phoD*- and *phoC*-harboring microbial communities and ALP/ACP activities, which reduces the release of P_{coll} into leachate. In addition, the manure biochar was more effective than the straw biochar in promoting competition and cooperation in the co-occurrence network (2–5% nodes increased on average), and the key taxa Proteobacteria and Cyanobacteria were identified as the dominant species of potential ALP/ACP activities and P_{coll} content. Our findings provide a novel understanding of biochar reducing P_{coll} loss from the phosphatase perspective by regulating the *phoD*- and *phoC*-harboring communities during DRW events.

Highlights

- Biochar reduced P_{coll} by 15.5–32.1% in leachate during DRW cycles.
- P_{coll} decreased with increasing *phoD*- and *phoC*-harboring microbial communities.
- Proteobacteria and Cyanobacteria were the key taxa driving P_{coll} content.

Keywords Drying and rewetting events, Alkaline/acid phosphatase, Microbial mechanism, Proteobacteria, Cyanobacteria

Handling editor: Xiaoyuan Yan.

*Correspondence:

Xinqiang Liang

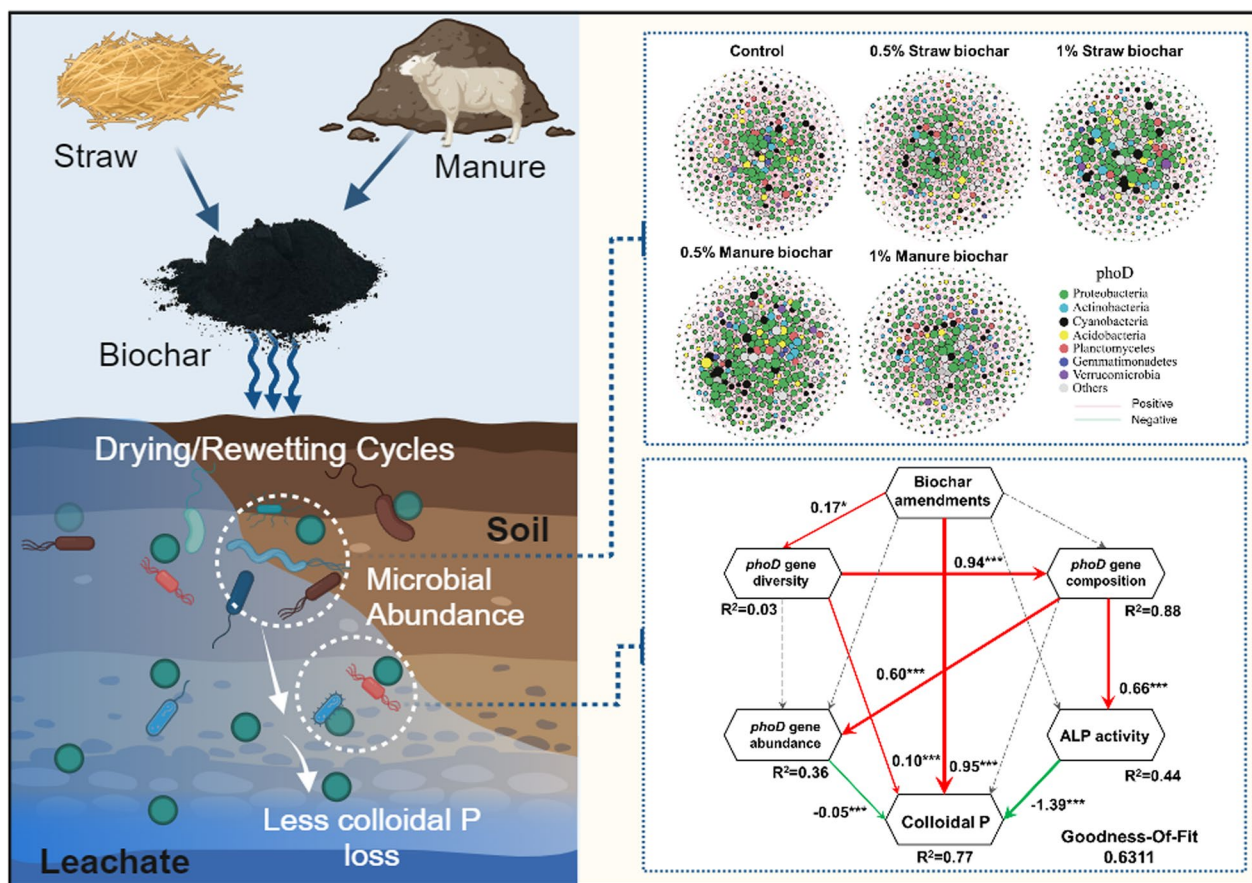
liang410@zju.edu.cn

Full list of author information is available at the end of the article



© The Author(s) 2023. **Open Access** This article is licensed under a Creative Commons Attribution 4.0 International License, which permits use, sharing, adaptation, distribution and reproduction in any medium or format, as long as you give appropriate credit to the original author(s) and the source, provide a link to the Creative Commons licence, and indicate if changes were made. The images or other third party material in this article are included in the article's Creative Commons licence, unless indicated otherwise in a credit line to the material. If material is not included in the article's Creative Commons licence and your intended use is not permitted by statutory regulation or exceeds the permitted use, you will need to obtain permission directly from the copyright holder. To view a copy of this licence, visit <http://creativecommons.org/licenses/by/4.0/>.

Graphical abstract



1 Introduction

Drying and rewetting (DRW) events are among the most prevalent environmental stresses that can significantly affect soil phosphorus (P) release, and lead to P loss from agricultural soils through leaching and runoff (Sun et al. 2017; Zhu et al. 2019). It is commonly believed that P exists as nano and colloidal particles (1–1000 nm) because the soil contains a richness of colloids with high specific surface area and charge, which have been proven to be P carriers in agricultural soils (Gu et al. 2020; Hens and Merckx 2002). Moreover, recent studies revealed that the released P during DRW events was derived from microbial cell lysis, which was also identified as colloidal P (P_{coll}) (Dinh et al. 2017). However, P_{coll} has low bioavailability and remains suspended in soil solution, contributing more to migration ability than settled particles (Yang et al. 2021a, 2021b). In general, P_{coll} in soil environmental systems is considered as a potential risk for surface water eutrophication

and has become a worldwide concern (Powers et al. 2016; Schindler et al. 2016).

Related studies have shown that the P released during DRW events is primarily in the form of organic P (Blackwell et al. 2009; Gu et al. 2018). A recent study reported that particulate organic P was the major specie in open bay waters, and colloidal organic P accounted for 33–65% (Yang et al. 2021a, 2021b). Therefore, P_{coll} may be affected by soil phosphatase, such as alkaline phosphatase (ALP) and acid phosphatase (ACP) (Sun et al. 2017; Wang et al. 2021a, 2021b, 2021c). Relevant research demonstrated that the enzymatic hydrolysis of organic P and death of microbial cells contributed at least 51% and 16% to the increase in Olsen-P during DRW events, respectively (Wang et al. 2021a, 2021b, 2021c). Similarly, DRW events increased soil phosphatase activity and increased soil available P by at least 37% (Novair et al. 2021). Moreover, a meta-analysis compiled from over 1800 observations summarized that the drying process decreased soil

enzymatic activities by 13–21%; and upon rewetting the dried soil, phosphatase activity increased by 12% (Gao et al. 2020). However, the relationship between P_{coll} and phosphatase-producing microorganisms during DRW events is limited by technique.

Since *phoD* gene (ALP encoded) specific primers have been developed by Sakurai, the contribution of microorganisms to ALP activity can be determined by detecting ALP encoded gene (Nannipieri et al. 2018; Sakurai et al. 2008). Recent studies have shown a positive correlation between ALP activity and *phoD*-harboring microbial communities (Chen et al. 2019a, 2019b; Tian et al. 2021). Furthermore, the *phoC* gene determines the ACP activity by microorganisms, which is considered superior to the ALP activity in soils with neutral or low pH (Fraser et al. 2017; Luo et al. 2019). However, soil phosphatase activity and phosphatase-producing microorganisms can also be affected by DRW events, which creates a knowledge gap between P migration and microbial response under environmental stress (Chen et al. 2021; Zhu et al. 2019). It is thus of great environmental significance to reveal the relationship between ALP/ACP and P_{coll} during DRW events from the genetic perspective.

Applying biochar has been shown to reduce P loss and regulate microbial composition (Wang et al. 2021a, 2021b, 2021c, 2023; Yang et al. 2021a, 2021b). For example, straw and manure biochar can effectively reduce the loss of soil P_{coll} by 55.2–56.7%; and the diversity of feedstocks results in different microbial cooperation and competition (Wang et al. 2023). Moreover, recent research has found that adding biochar can enhance soil phosphatase activity and decrease P loss (Yang and Lu 2022). The potential explanations for this mechanism are as follows: (i) the adsorption/desorption capacity of soil P is altered by enhancing the soil characteristics such as soil aggregates (Islam et al. 2021; Xu et al. 2014); (ii) the large specific surface area of carbon frames provides shelter for microorganisms and enhances their resistance to DRW stress, relieving cell lysis and microbial P release (Yang et al. 2023); (iii) the biochar feedstocks provide the soil with labile carbon, which can effectively associate with soil P (Huang et al. 2021). Nevertheless, there are few reports to comprehensively evaluate the response of P_{coll} and phosphatase activity during DRW events under different biochar addition strategies.

In this study, we performed a DRW platform to investigate the potential effects of different biochar strategies on P_{coll} content in leachate and soil microbial mechanisms. Specifically, the objectives were to (1) evaluate the effect of biochar addition on mediating the content of P_{coll} ; (2) explore the microbial mechanism from ALP/ACP activity, and *phoD*/*phoC*-harboring microbial community; and (3) identify key taxa species and their possible links.

2 Materials and methods

2.1 Soil sampling and biochar preparation

Top soil samples (0–20 cm) were collected from Pinghu Environmental Monitoring Station (soil A), Jiaxing City (120° 23′ 47″ E, 29° 44′ 09″ N) and Tiantai Environmental Monitoring Station (soil B), Taizhou City (120° 50′ 33″ E, 29° 7′ 38″ N), Zhejiang Province, China. The soil textures of soil A and B are silty loam and clay loam, respectively (United States Department of Agriculture, USDA). The soil sample was air-dried, and passed through a 2-mm mesh after manually removing all visible non-soil materials. Then, the soil sample was stored at 5 °C for further experiment.

The agricultural residues (rice straw and cattle manure) were collected locally for biochar production. Briefly, about 100 g air-dried feedstock was placed in a muffle furnace (QT-2.5-10, Suzhou Qiantong Instrument Equipment Co. Ltd., China), and heated to 400 °C at a rate of 8 °C min⁻¹ with a residence time of 2 h under oxygen-limited conditions using the slow pyrolysis method (Safari et al. 2020). After cooling to room temperature, the biochar was removed and sieved through a 5-mm mesh. The basic physicochemical properties of the two soils and used biochar are presented in Additional file 1: Table S1.

2.2 Experimental design

To perform the leaching experiment, soil columns were made of acrylic glass with a length of 40 cm and an inner diameter of 10 cm. Each column was filled with about 2 kg of air-dried soil and treated as follows: (1) control without biochar addition (CK); (2) straw biochar addition rate of 0.5% (SBL); (3) straw biochar addition rate of 1.0% (SBH); (4) manure biochar addition rate of 0.5% (MBL); and (5) manure biochar addition rate of 1.0% (MBH). The soil columns were sealed, each with a rubber plug with a hole pierced in the middle. Deionized water (18.2 MΩ cm, Millipore) was used as the influent solution and injected with a soft hose. The leachate was discharged via a peristaltic pump. The bottom of the column was filled with quartz sand and gauze to prevent soil from clogging the water outlet. Three replicates were established for each treatment.

Each treatment ran through three consecutive DRW cycles (named cycle-1, -2, and -3) (Blackwell et al. 2009). The leaching rate was maintained at 1.5 ml min⁻¹. After each leaching for 10 h, the peristaltic pump was disconnected, and the soil was then gradually dried by flushing N₂ (90 L h⁻¹, 25 ± 2 °C) until it reached a constant weight. The soil was air-dried within 3 days before the next leaching stage, regarded as completing the first DRW cycle (Gu et al. 2018). Soil samples were collected after the third DRW cycle. A portion was used for soil physicochemical

property analysis; and the frozen soil samples ($-80\text{ }^{\circ}\text{C}$) for DNA extraction.

2.3 Soil chemical and biological analyses

Soil pH was measured in a 1:5 (w:v) soil/water suspension using a pH meter (PHS-3 C, Shanghai, China). Soil total carbon (TC) and total nitrogen (TN) were determined using an Elemental Analyzer (Vario MAX CNS, Elementar, Germany). Soil total P was measured by $\text{H}_2\text{SO}_4\text{-HClO}_4$ digestion, followed by the molybdenum blue colorimetry (Walker and Adams 1959). Cation exchange capacity (CEC) was measured as described by Gaskin et al. (2008). Soil texture was measured using the hydrometric method (Li et al. 2020). The P_{coll} concentration was determined as described by Pagel et al. (2008). Briefly, the leachate (i.e., Sample I) was centrifuged at $3000\times g$ for 10 min, after which the supernatant was filtered through 1000 nm filter paper (Millipore Amicon, Ultra, USA; Sample II). And then the leachate was centrifuged at $4000\times g$ for 45 min using a membrane with a pore size of 3 kDa (Millipore Amicon, Ultra, USA; Sample III) to represent the particle size <1 nm. The particulate P (PP, >1000 nm), P_{coll} (1–1000 nm), and truly soluble P (TSP, <1 nm) were calculated based on the difference between the P concentration of Samples I, II, and III (Eltohamy et al. 2021). The total dissolved P (TDP) was the sum of PP, P_{coll} , and TSP.

The detection of ALP and ACP activities was described by Tabatabai and Bremner (1969). In brief, ALP and ACP were cultured in the buffer solution with pH 6.5 and 11, respectively, and then *p*-nitrophenyl phosphate (PNP) was used as a substrate. Enzyme activities were considered to be the amount of *p*-nitrophenol produced by 1 g of soil per hour.

2.4 Soil DNA and qPCR quantification

The total soil DNA was extracted from 0.5 g of frozen soil using the DNeasy PowerSoil Kits (Qiagen, Hilden, Germany). The DNA purity was determined by NanoDrop ND-2000 spectrophotometer (Thermo Scientific Wilmington, DE, USA), and then tested with 1% (w/v) agarose gels.

The *phoD* and *phoC* gene abundances were determined by quantitative polymerase chain reaction (qPCR) using a QuantStudio 3 Real-time PCR System (Applied Biosystems, Foster City, CA, USA). The primer pairs amplifying *phoD* and *phoC* genes were ALPS-F730 (5'-CAG TGGGACGACCACGAGGT-3')/ALPS-R1101 (5'-GAG GCCGATCGGCATGTCG-3') (Sakurai et al. 2008); and *phoC*-A-F1 (5'-CGGCTCCTATCCGTCCGG)/*phoC*-A-R1 (5'-CAACATCGCTTTGCCAGTG) (Fraser et al. 2017). The PCR was run in triplicate using 20 μL reactions comprising 10 μL $2\times$ Taq MasterMix, 1 μL of each

primer (10 μM), 1 μL template DNA, and 7 μL of ddH₂O. The cycling conditions were 95 $^{\circ}\text{C}$ for 3 min, followed by 40 cycles at 95 $^{\circ}\text{C}$ for 15 s, 60 $^{\circ}\text{C}$ for 15 s, 72 $^{\circ}\text{C}$ for 20 s, and 60 $^{\circ}\text{C}$ for 1 min. The triplicate PCR products were then purified using the AxyPrep DNA Gel Extraction Kit (Axygen, Hangzhou, China). The standard curve was constructed using 10-fold dilution sequences of linearized plasmids containing target genes.

2.5 Illumina sequencing and sequence analysis

Sequencing was performed on the Illumina MiSeq 2000 platform by Biomarker Technologies Corporation (Beijing, China). The raw sequencing data were performed by the UCluster method in QIIME2 (<https://qiime2.org/>), and the RDP FunGene pipeline (Bolyen et al. 2019; Fish et al. 2013). Briefly, the overlapping counterpart reads were assembled and the primer sequence was removed. The *phoD* gene sequences of 200–350 bp length (about 2% discarded), and *phoC* gene sequences of 100–175 bp length (about 2% discarded) were retained. And then the non-corresponding sequence of *phoD/phoC* was removed through the RDP FunGene pipeline. In total, 1,116,735 (*phoD*) and 1,140,791 (*phoC*) high-quality sequences were obtained. The *phoD* and *phoC* purified sequences in each sample were assigned to the operational taxon with a similarity of 80% and 88%, respectively (Luo et al. 2019). Maximum-likelihood phylogeny was calculated by MEGA 7 and visualized using the iTOL webserver (<http://itol.embl.de/>). The original DNA sequences have been uploaded to the National Center for Biotechnology Information and registered with the BioProject ID number: PRJNA911733 (<https://www.ncbi.nlm.nih.gov/bioproject/911733>).

2.6 Statistical analysis

Unless otherwise indicated, one-way analysis of variance (ANOVA), followed by least significant difference (LSD) was performed using SPSS software (version 21) to compare means for each variable ($p < 0.05$). Principal coordinate analysis (PCoA) was performed using the “vegan” package to explore dissimilarity based on Bray-Curtis distances (Wang et al. 2018).

Network analyses were performed at the operational taxonomic units (OTU) level using the Spearman correlation matrix (Wei et al. 2019); and correlation coefficients were calculated using the “psych” package (Yan et al. 2021). The error discovery rate correction was performed using the Benjamini-Hochberg procedure, keeping the merged edges with p -values < 0.05 (Benjamini and Hochberg 1995). Moreover, the final networks were visualized by Gephi software (version 9.0.2) (Jacomy et al. 2014).

A partial least-squares path model (PLSPM) was established to quantify the contribution of phosphatase activity (ALP, ACP), gene copy numbers (*phoC*, *phoD*), microbial alpha diversity (Chao 1, ACE, Simpson, and Shannon index), and P_{coll} content using the R package “plsrm” (Wang et al. 2023).

3 Results

3.1 Distribution of P in leachate during DRW events

DRW produced the initial peak of P concentration in the leachate of the two tested soils (A and B), which then gradually decreased until the end of the leaching cycle (Table 1). TDP concentrations in the leachate of both soils decreased significantly from cycle-1 to

cycle-3 ($F = 11.9$, $p < 0.05$ for soil A; $F = 13.4$, $p < 0.05$ for soil B). As a result, the TSP and PP of the biochar treatments (i.e., SB and MB) were always greater than those of the control. However, the biochar addition resulted in a significant decrease in P_{coll} concentration from the beginning to the end of the leaching cycle in both soil A and B ($F = 5.8$, $p < 0.05$), with no significant difference between the biochar treatments. Consequently, biochar addition during the three DRW cycles reduced the P_{coll} release from soil A by 17.6–32.1% and from soil B by 15.5–17.6%, compared to the CK. Notably, the P_{coll} concentration in the leachate of soil A was significantly lower than that of soil B ($F = 63.1$, $p < 0.001$), indicating

Table 1 Phosphorus distribution in leachate during DRW cycles

Soils	DRW cycles	Treatments	Phosphorus distribution ($\mu\text{g L}^{-1}$)			
			P_{coll}	PP	TSP	TDP
Soil A	Cycle-1	CK	103 ± 10	69 ± 5	246 ± 9	418 ± 15
		SBL	72 ± 4	92 ± 4	364 ± 32	528 ± 47
		SBH	94 ± 2	164 ± 9	712 ± 66	970 ± 82
		MBL	83 ± 4	125 ± 10	455 ± 19	663 ± 41
		MBH	92 ± 5	172 ± 14	954 ± 61	1218 ± 96
	Cycle-2	CK	91 ± 8	61 ± 3	236 ± 10	388 ± 13
		SBL	54 ± 10	76 ± 9	305 ± 24	435 ± 38
		SBH	76 ± 7	118 ± 14	538 ± 50	732 ± 68
		MBL	63 ± 9	103 ± 6	394 ± 17	560 ± 36
		MBH	70 ± 6	129 ± 11	751 ± 45	950 ± 71
	Cycle-3	CK	85 ± 8	55 ± 3	249 ± 25	389 ± 14
		SBL	49 ± 9	58 ± 9	309 ± 33	416 ± 36
		SBH	62 ± 5	89 ± 7	382 ± 20	533 ± 55
		MBL	61 ± 6	70 ± 7	316 ± 36	447 ± 33
		MBH	58 ± 7	81 ± 3	446 ± 14	585 ± 56
Soil B	Cycle-1	CK	198 ± 1	84 ± 4	256 ± 19	538 ± 23
		SBL	133 ± 18	101 ± 7	341 ± 12	575 ± 13
		SBH	182 ± 6	155 ± 6	782 ± 20	1119 ± 17
		MBL	151 ± 6	119 ± 6	428 ± 7	698 ± 15
		MBH	186 ± 2	171 ± 6	1017 ± 129	1374 ± 147
	Cycle-2	CK	143 ± 16	90 ± 8	237 ± 9	470 ± 10
		SBL	97 ± 6	66 ± 9	347 ± 38	510 ± 11
		SBH	119 ± 5	70 ± 8	516 ± 51	705 ± 5
		MBL	111 ± 8	71 ± 6	361 ± 5	543 ± 9
		MBH	126 ± 4	83 ± 15	722 ± 81	931 ± 96
	Cycle-3	CK	128 ± 7	81 ± 4	217 ± 14	426 ± 15
		SBL	81 ± 7	41 ± 8	326 ± 40	448 ± 8
		SBH	101 ± 5	55 ± 5	384 ± 21	540 ± 6
		MBL	94 ± 4	54 ± 6	334 ± 53	482 ± 9
		MBH	109 ± 6	64 ± 7	407 ± 76	580 ± 86

P_{coll} colloidal P, PP particulate P, TSP truly soluble P, TDP total dissolved P, CK no biochar addition, SBL 0.5% straw biochar addition, SBH 1% straw biochar addition, MBL 0.5% manure biochar addition, MBH 1% manure biochar addition. Values are the means standard errors ($n = 3$)

that P_{coll} in the weakly acidic soil leaching may be greater than that in the weakly alkaline paddy soil.

3.2 Phosphatase activities and *phoD*/*phoC* genes abundance

Compared to CK, adding biochar increased the potential ALP activities by 7.7–15.1% in soil A and 17.1–49.1% in soil B after the three DRW cycles (Fig. 1a). By contrast, the ACP activities in soil A decreased by 7.3–32.9% after the biochar addition, and they varied between –26.2% and 18.5% in soil B (Fig. 1b), because biochar inhibited ACP activity in alkaline soil. The variation trend of *phoD* and *phoC* genes abundance was similar to that of ALP and ACP activity (Fig. 1c, d). Generally, the biochar addition contributed to the increase in ALP activity and *phoD* gene abundance ($p < 0.05$), and the decrease in ACP activity and *phoC* gene abundance ($p < 0.05$). There was a significant difference in ACP activity and *phoC* gene

abundance between the tested treatments ($p < 0.05$), whereas ALP activity and *phoD* gene abundance remained relatively stable. In addition, ALP activity was positively correlated with *phoD* gene abundance in the two soils ($R^2 = 0.514$, $p < 0.05$ for soil A, and $R^2 = 0.713$, $p < 0.05$ for soil B) (Fig. 2a). And the same trend of correlation was found between the ACP activities and the *phoC* gene abundance ($R^2 = 0.579$, $p < 0.05$ for soil A, and $R^2 = 0.702$, $p < 0.05$ for soil B) (Fig. 2b). In addition, the P_{coll} was significantly negatively correlated with the phosphatase activity and the gene abundance ($p < 0.05$) in both soils (Fig. 2c–f).

3.3 *PhoD*- and *phoC*-harboring microbial abundance and community structure

The phylogenetic relationship between *phoD*- and *phoC*-harboring microbial communities was established at the OTU levels (Fig. 3). The OTU diversity may encode

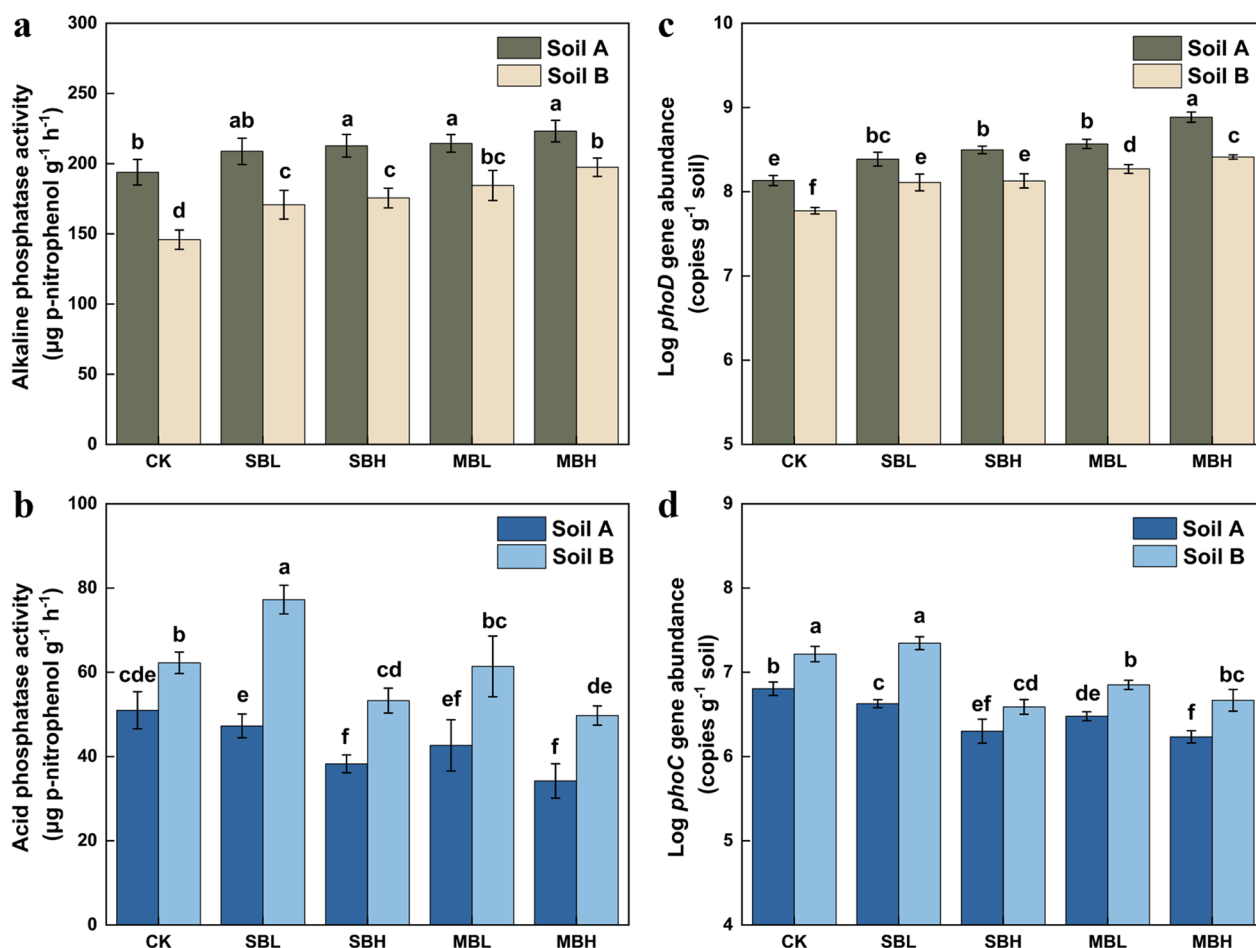


Fig. 1 Soil alkaline phosphatase (ALP) activities (a), the abundance of the *phoD* gene estimated by the gene copy numbers (b), acid phosphatase (ACP) activities (c), and abundance of the *phoC* gene estimated by the gene copy numbers (d). Different letters indicate significant differences between treatments ($p < 0.05$). Error bars were calculated from triplicate experiments conducted in parallel on the same soil. CK no biochar addition, SBL 0.5% straw biochar addition, SBH 1% straw biochar addition, MBL 0.5% manure biochar addition, MBH 1% manure biochar addition

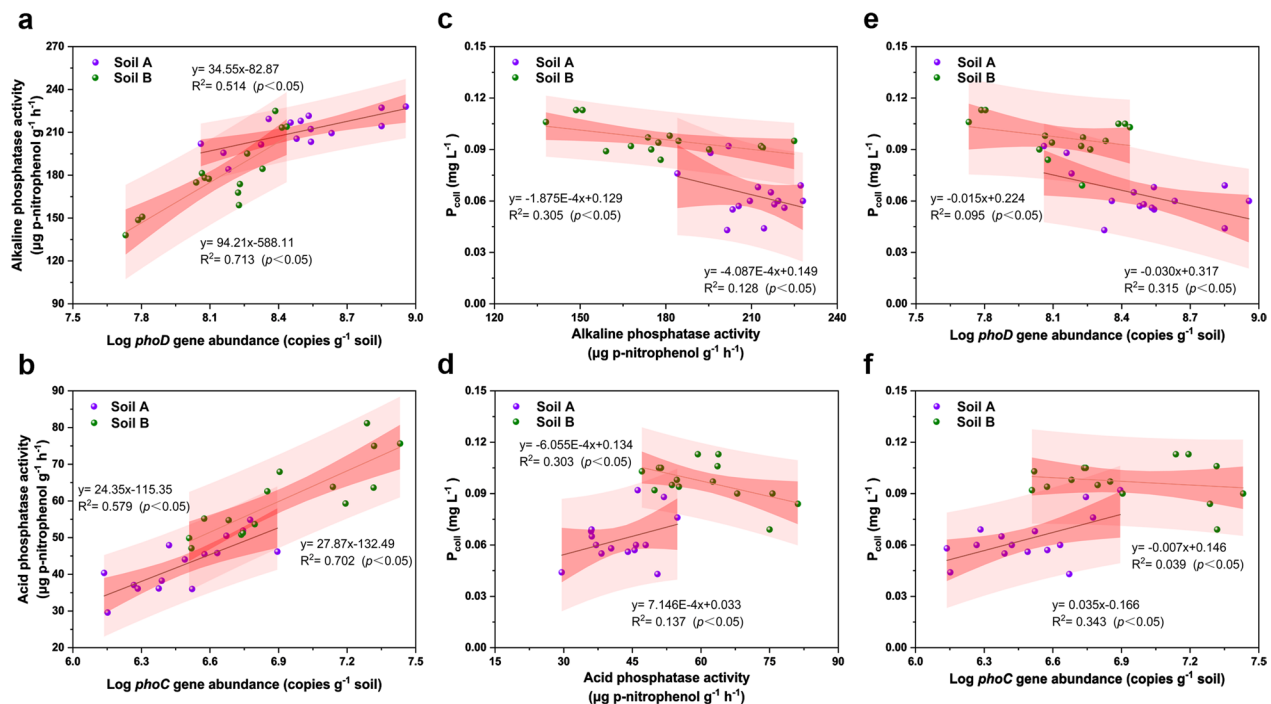


Fig. 2 Relationships between alkaline/acid phosphatase activities and the abundances of *phoD/phoC* genes and colloidal phosphorus (P_{coll})

different *phoD*- and/or *phoC*-harboring microbial communities; at the same time, any one phyla may also encode multiple OTUs. The predominant phylum of *phoD* gene was Proteobacteria, Actinobacteria, Cyanobacteria, Firmicutes, Deinococcus-Thermus, Gemmatimonadetes, and Planctomycetes; the superior phylum within *phoC*-harboring was Proteobacteria and Cyanobacteria.

The alpha diversity of *phoD*- and *phoC*-harboring microbial communities were characterized by ACE, Chao1, Shannon, and Simpson diversity indices (Table 2). Variation in all beta diversity indices variation was affected by soil type and biochar addition (Additional file 1: Fig. S1). Specifically, two principal coordinates fully explained 52.02% ($R^2 = 0.247$, $p = 0.008$) and 37.98% ($R^2 = 0.317$, $p = 0.001$) of the variation in *phoD*- and *phoC*-harboring microbial communities, respectively.

The networks showed that *phoD*-harboring species (Fig. 4a) were more closely connected than *phoC*-harboring species (Fig. 4b) in both the control group and biochar addition groups. We found a 1.5-fold increase in node number after biochar addition in *phoC*-harboring species; in contrast, there was no significant change in *phoD*-harboring species, suggesting biochar addition could lead to more conflicting interactions among the *phoC*-harboring species (Additional file 1: Table S2). In addition, seven phyla of these OTUs were observed in

the *phoD*-harboring species, belonging to Proteobacteria, Actinobacteria, Cyanobacteria, Acidobacteria, Planctomycetes, Gemmatimonadetes, and Verrucomicrobia. Similarly, the OTU59, 90, and 206 were identified in the *phoC*-harboring species, which were considered the keystone with more edges, and further analyzed related to Proteobacteria, Cyanobacteria, and Bacteroidetes.

3.4 Relationship between phosphatase activities, *phoD*- and *phoC*-harboring microbial communities, and P_{coll}

The structural equation model (SEM) revealed that the biochar addition decreased P_{coll} through multiple pathways on phosphatase and related genes (Fig. 5). Specifically, there was a direct positive correlation between biochar addition and P_{coll} in the leaching solution, but finally a negative correlation for regulating ALP and ACP and *phoD* and *phoC*-harboring microorganisms. Regarding phosphatase activity, biochar addition displayed a stronger impact on P_{coll} in ALP (0.95) than in ACP (0.64). At the same time, there was a positive correlation between the abundance of functional genes, composition, diversity, and the activity of the related enzymes. Overall, biochar addition altered P_{coll} in the leachate mainly through regulating *phoD*- and *phoC*-harboring microbial communities.

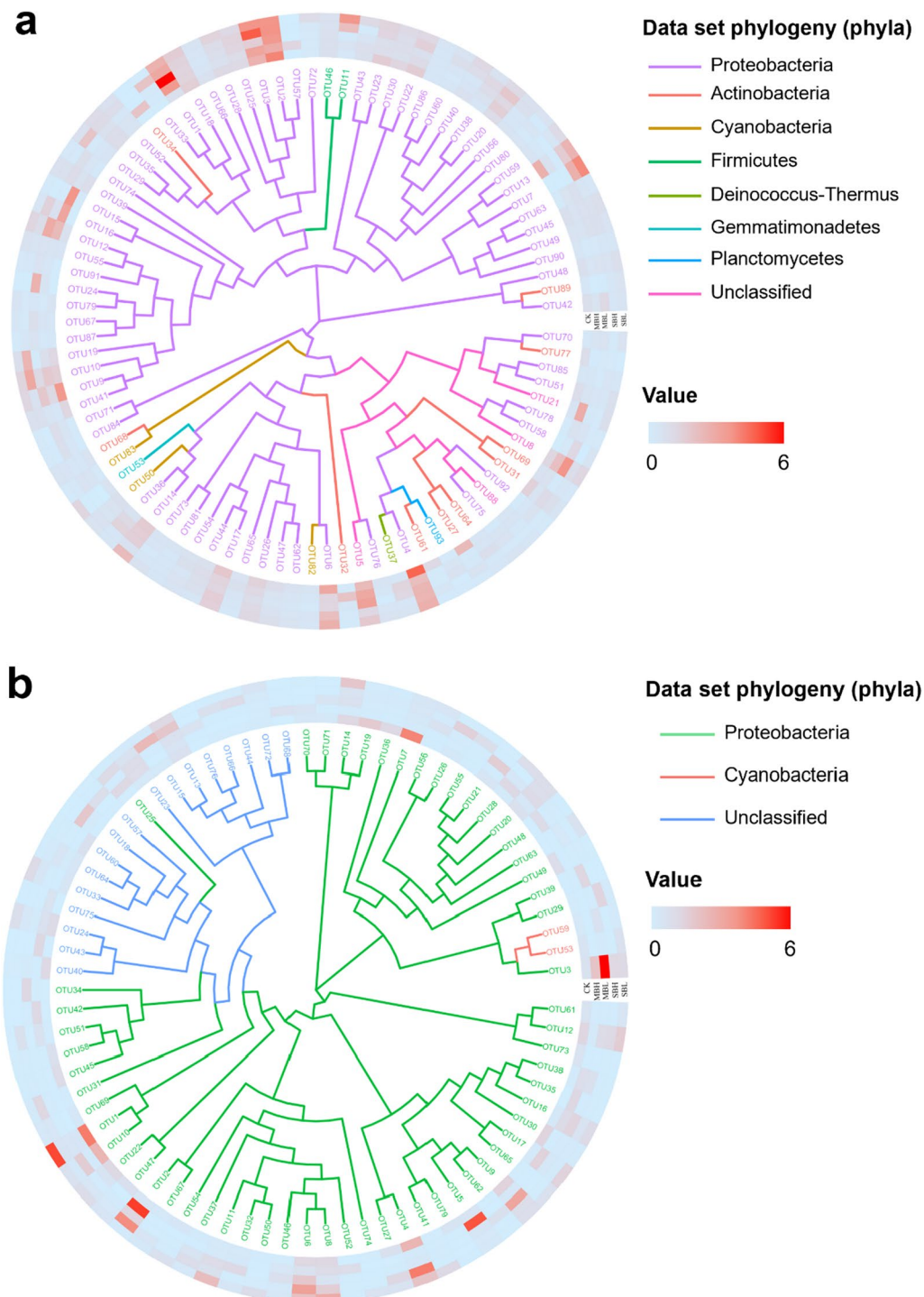


Fig. 3 Phylogenetic relationships among the *phoD*- (a) and *phoC*-harboring (b) microbial communities based on OTU abundance (mean related abundance > 0.1%). Leaf labels indicate representative sequence IDs (OTU). The colors of the branches and OTU represent different taxonomies of the sequences based on the phyla and genus level taxonomy, respectively. Rings from the inner to the outside circles represent the relative abundance of OTU in different treatments. CK no biochar addition, SBL 0.5% straw biochar addition, SBH 1% straw biochar addition, MBL 0.5% manure biochar addition, MBH 1% manure biochar addition

Table 2 Alpha diversity indices of the soil microbial community

Soil A	ACE	Chao1	Shannon	Simpson	Soil B	ACE	Chao1	Shannon	Simpson
<i>phoD</i> -harboring microbial group									
CK	835.39 ± 74.80ab	821.22 ± 82.07ab	5.53 ± 0.08b	0.06 ± 0.00a	CK	541.71 ± 78.02a	541.47 ± 79.36a	4.06 ± 0.34ab	0.15 ± 0.04a
SBL	862.11 ± 23.67a	871.42 ± 43.12a	5.84 ± 0.46ab	0.05 ± 0.01a	SBL	547.67 ± 40.41a	564.05 ± 52.23a	4.33 ± 0.58ab	0.13 ± 0.06a
SBH	840.23 ± 49.51a	844.25 ± 51.26ab	5.71 ± 0.09a	0.06 ± 0.00a	SBH	429.20 ± 15.28b	417.90 ± 35.66b	3.82 ± 0.22b	0.14 ± 0.02a
MBL	767.43 ± 12.15b	780.04 ± 27.45b	5.88 ± 0.39ab	0.04 ± 0.00b	MBL	591.22 ± 89.37a	590.59 ± 84.06a	4.47 ± 0.31a	0.15 ± 0.03a
MBH	907.14 ± 55.57a	928.42 ± 77.85a	6.19 ± 0.41a	0.03 ± 0.01b	MBH	630.12 ± 53.50a	646.59 ± 41.64a	4.37 ± 0.12a	0.10 ± 0.00a
<i>phoC</i> -harboring microbial group									
CK	120.56 ± 6.33a	117.97 ± 8.77a	3.03 ± 0.54ab	0.18 ± 0.06c	CK	120.26 ± 6.75ab	115.92 ± 6.13a	3.04 ± 0.27a	0.19 ± 0.02b
SBL	103.10 ± 4.36b	101.62 ± 4.70b	3.66 ± 0.25a	0.13 ± 0.02c	SBL	91.09 ± 6.92c	86.29 ± 7.37b	2.51 ± 0.34ab	0.40 ± 0.06a
SBH	77.32 ± 1.83c	77.50 ± 6.73c	2.61 ± 0.25ab	0.24 ± 0.05b	SBH	116.10 ± 13.88ab	120.47 ± 13.87a	2.45 ± 0.34b	0.31 ± 0.08a
MBL	63.37 ± 4.30d	65.40 ± 10.62c	2.09 ± 0.26c	0.44 ± 0.06a	MBL	122.57 ± 5.94a	121.99 ± 9.64a	1.99 ± 0.20b	0.47 ± 0.11a
MBH	61.48 ± 14.72d	58.67 ± 13.51c	1.62 ± 0.41c	0.52 ± 0.09a	MBH	97.45 ± 16.63bc	98.08 ± 14.40ab	2.05 ± 0.28b	0.38 ± 0.01a

CK no biochar addition, SBL 0.5% straw biochar addition, SBH 1% straw biochar addition, MBL 0.5% manure biochar addition, MBH 1% manure biochar addition. Values are the means standard errors ($n = 3$). Different letters denote significant differences ($p < 0.05$)

4 Discussion

4.1 Biochar addition inhibited the release of P_{coll} under DRW cycles

The concentration of all P-fractions in the leaching solution was reduced in both tested soils during DRW cycles (Table 1). It is worth noting that the biochar addition consistently resulted in decreased P_{coll} concentrations compared to the control. This may be related to the physical behavior of P adsorption and increased organic carbon by biochar (Li et al. 2022). Although in this study we focused on the effect of biochar on P_{coll} mineralization from the view of the microbial enzymatic hydrolysis, we could not ignore that direct biochar itself directly adsorbed P, and indirectly affected the adsorption of P_{coll} by regulating soil characteristics. On the one hand, the porous structure of biochar surface can adsorb P_{coll} and provide suitable habitats for microorganisms to improve their environmental resistance, and avoid releasing colloidal-bond P from dead microbial cell lysis (Palansooriya et al. 2019). On the other hand, biochar addition increases soil pH, thus increasing P_{coll} adsorption efficiency. This may be because the protonated hydroxyl ($-OH$) groups on the biochar surface were negatively charged, and the P_{coll} was desirable for the adsorption by electrostatic attraction (Yang et al. 2019). Moreover, several studies suggested the P released during the DRW events could also be attributed to the changes in soil pH, as Fe/Al oxides affect P adsorption capacity, which is pH-sensitive (Hens and Merckx 2001; Turner et al. 2003). In our study, the biochar showed satisfactory adsorption properties for P_{coll} under weakly alkaline conditions, and a reasonable explanation for this phenomenon is that chemisorption through the formation of inner-sphere complexation was the dominant adsorption process (Yan et al. 2022).

We also compared the surface functional groups of the two types of biochar by FTIR spectroscopy (Additional file 1: Fig. S2). Specifically, we observed abundant surface functional groups, such as $-OH$ stretching vibration at around 3390 cm^{-1} belonging to hydroxyl groups; the aromatic skeletal $C=C$ vibrations at 1642 and 1420 cm^{-1} ; the $M-O$ and $O-M-O$ ($M=Mg, Al$) vibration weak appearing in the $456-820\text{ cm}^{-1}$ region; and $C=O$ stretching vibration at 1090 cm^{-1} mainly associated with carboxyl, trace of aldehydes, and ketones (Feng et al. 2023; Jiang et al. 2020; Yang et al. 2023). And it should be noted that the only difference between straw biochar and manure biochar was the peak at 2823 cm^{-1} , which is usually considered as $-CH_2$, assigning to nonpolar aliphatic fractions in biopolymer (Han et al. 2017). Therefore, we believe that organic carbon in manure biochar is more easily metabolized by microorganisms, which is one of the main reasons for attracting more phosphatase functional microorganisms. As reported in our previous research, C_{mic} and P_{mic} were considered as indicators to link soil properties and microbial communities, and biochar addition increased C_{mic} and P_{mic} , suggesting that the overall soil microbial abundance improved, which led part of the P_{coll} to be absorbed and utilized by microorganisms (Wang et al. 2023). Overall, the inhibition mechanism of biochar on P_{coll} loss potential is a comprehensive result, including its direct adsorption effect and indirect regulation of soil properties and phosphatase function microbial community. Field-scale experiments also confirmed this result, and the mechanism is mainly based on physical sorption (Wang et al. 2021a, 2021b, 2021c).

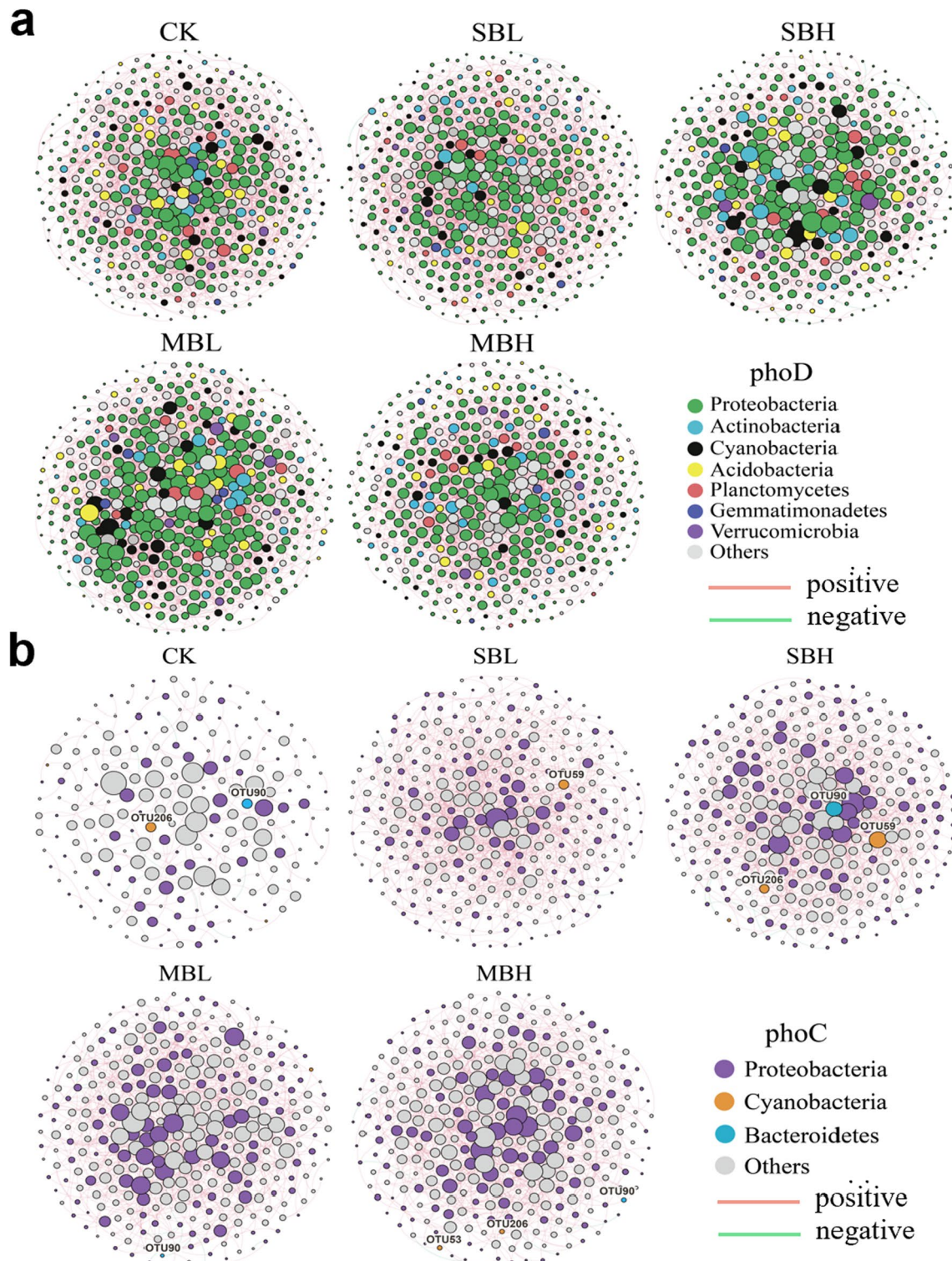


Fig. 4 Co-occurrence networks between the *phoD*- (a) and *phoC*-harboring (b) microbial communities based on OTU abundance (mean related abundance > 0.1%), and each connection represents a very strong (Spearman's $R > 0.6$) and significant ($p < 0.01$) correlation. Red lines indicate significant positive correlations, and blue lines represent significant negative correlations. CK no biochar addition, SBL 0.5% straw biochar addition, SBH 1% straw biochar addition, MBL 0.5% manure biochar addition, MBH 1% manure biochar addition

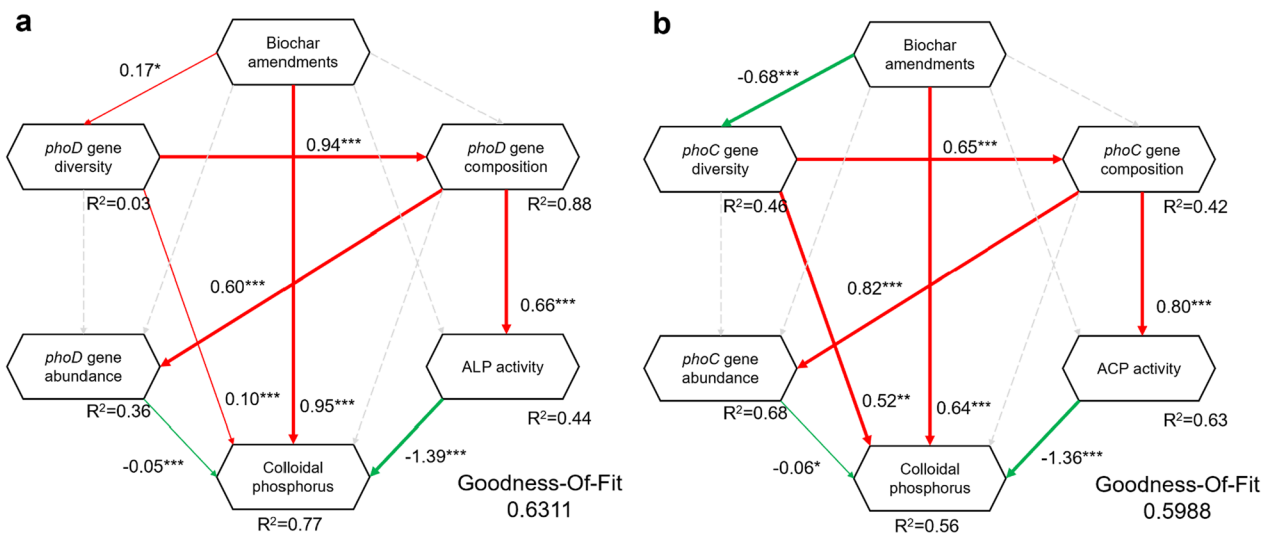


Fig. 5 Structural equation model (SEM) showing the relationships between biochar amendments, *phoD* (a) and *phoC* (b) gene diversity, abundance, and composition, phosphatase activity (ALP and ACP) on colloidal phosphorus. Green arrows indicate negative effects, red arrows indicate positive effects, and dashed arrows indicate non-significant paths, which were removed in the final model. Arrow widths illustrate the strength of the standardized path coefficient, and R^2 values represent the proportion of the variance explained for each endogenous variable. Significance levels are indicated by "*" ($p < 0.05$), "***" ($p < 0.01$), and "****" ($p < 0.001$) levels

4.2 Biochar addition regulated phosphatase activities and *phoD*- and *phoC*-harboring microbial communities

At the same time, numerous studies have confirmed that phosphatase activities were closely associated with P forms and composition (Luo et al. 2019; Tian et al. 2021; Wei et al. 2019). Our results further suggested that P_{coll} may be present as organic P and can be affected by phosphatase. It has also been shown that colloidal organic P can be stable with Fe (III) in soil solution and consequently contribute to plant acquisition; our results provide evidence for the bioavailability of P_{coll} from the enzymatic perspective (Bollyn et al. 2017). Interestingly, ACP activity was positively correlated with P_{coll} in weakly alkaline soil, which could be because some ACPs were stable in the soil colloids (Gao and DeLuca 2018). This phenomenon reflects that the alkaline soil with biochar may reduce the stability and persistence of ACP (Renella et al. 2006). Nevertheless, the structural equation model showed that P_{coll} was ultimately negatively correlated with soil phosphatase activity under biochar addition. This may be because ALP played a key role in the P_{coll} content rather than ACP. On the other hand, we found that both ALP and ACP activities were affected by the initial soil pH value, and the ACP activity was sensitive to biochar addition in acidic soil (Tian et al. 2021).

We examined the *phoD*- and *phoC*-encoding microbial communities to measure the ALP and ACP activity. And the Proteobacteria and Cyanobacteria were identified with potential ACP and ALP activities in both *phoD*- and *phoC*-harboring species (Luo et al. 2019). This is

because phosphatase genes could exist in multiple copies, and different species could also produce similar genetic sequences and then encode phosphatase (Gaiero et al. 2018). Therefore, it is not only *phoD*- and *phoC* gene abundance but also the community composition encoded by the genes that cooperatively determine phosphatase production; and contribute to P mobilization (Bergkemper et al. 2016). Furthermore, keystone species, such as Proteobacteria, play a key role in both *phoD*- and *phoC*-harboring microbial communities, which was performed by network analysis (Wei et al. 2019). The *phoD*-harboring species exhibited a higher relative abundance and had more complex connections (e.g. nodes, edges, and graph density) than the *phoC*-harboring species. This is probably due to the *phoD*-coding gene having a richer species database (Fraser et al. 2017). In contrast, biochar amendment increased the network density of *phoD*- and *phoC*-harboring communities (Ma et al. 2020; Wang et al. 2023). Bello et al. (2020) reported a similar result that straw biochar resulted in a more complex connection than in soil without biochar. This could be due to the fact that biochar containing labile carbon substrates promotes the growth of microbial communities (Chigineva et al. 2009; Spohn and Kuzyakov 2013). Also, we observed that the density of the co-occurrence network varied under different biochar addition, which may be related to the feedstocks (Palansooriya et al. 2019). Similarly, Wang et al. (2023) reported that manure biochar was more effective

than straw biochar in promoting competition and cooperation in the co-occurrence network. This phenomenon could be explained by two possible reasons. On the one hand, compared to straw biochar, manure biochar contains more labile carbon, which can be considered a source of microbial nutrients. In contrast, large amounts of labile carbon require more microbial cooperation to be metabolized (Chen et al. 2019a, 2019b). At the same time, the higher abundance of microbial communities, in turn, caused “P starvation” which reflects the actual potential supply of phosphate for microorganisms (Bergkemper et al. 2016). Due to P limitations, the relative abundance of phosphatase functional microbes increases and enhances both competition and cooperation among their microbial communities to mineralize more P_{coll} to obtain available P for survival (Heuck et al. 2015). Many existing studies have observed that the abundance of soil nutrients such as carbon and phosphorus is a key factor causing competition and cooperation among microorganisms, which supports our view (Heuck et al. 2015; Luo et al. 2019; Wei et al. 2019).

4.3 Potential interactions between P_{coll} and *phoD*- and *phoC*-harboring microbial communities

According to the structural equation model, the P_{coll} can be directly affected by biochar amendments, and regulated by both *phoD*- and *phoC*-harboring microbial communities (Fig. 5). A positive relationship has been found between biochar and P_{coll} in the leachate, as it contains colloidal particles itself (Yang et al. 2020). However, the microbial indicators, particularly for ALP and ACP activities, displayed a dominant role in regulating P_{coll} in leachate. Our results indicate the expression of ALP and ACP by key species such as Proteobacteria can contribute to P_{coll} content (Luo et al. 2019; Wang et al. 2023; Wei et al. 2019). Although we did not specifically track the change in pH, it is reasonable to assume that biochar addition would increase the value of pH and thus the P_{coll} content. Recent studies showed that soil pH is a key environmental factor for microorganisms and determines the functional microbial community composition (Bi et al. 2020; Ragot et al. 2016). In fact, changes in soil carbon were key environmental predictors on the potential influence on both nutrient availability as well as certain microbial taxa, abundance, and functional population composition (Aanderud et al. 2018). Microbial phosphatases are involved in organic P mineralization to promote the availability of P and C from organo-phosphorylated compounds (Heuck et al. 2015). Thus, phosphatase activities can be driven by the microbial need for carbon. The *phoD*- and *phoC*-harboring microbial populations directly mediate the relationship between microbial communities and ACP/ALP activities. These

interactive effects may explain why the present study identified that *phoD*- and *phoC*-harboring populations were increased by the amendment of biochar. In general, our findings imply that biochar addition increased the *phoD*- and *phoC*-harboring communities, considerably reducing P_{coll} in the leaching solution.

5 Conclusions

In this study, we evaluated the effects of different biochar addition on P_{coll} released into leachate from the perspective of ALP/ACP activities and *phoD*- and *phoC*-harboring microbial communities during DRW events. Our results demonstrated that the biochar addition significantly decreased P_{coll} content during three DRW cycles. We also observed Proteobacteria and Cyanobacteria were the key taxa in *phoD*- and *phoC*-harboring microbial communities, in which, manure biochar performed more competition and cooperation than straw biochar. More importantly, we revealed that ALP/ACP activities were the key factors in inhibiting the release of P_{coll} under biochar addition through an established structural equation model. Our results provide a microbial mechanism for biochar controlling the migration and loss of P_{coll} during DRW events, which has great environmental and bioecological significance.

Supplementary Information

The online version contains supplementary material available at <https://doi.org/10.1007/s42773-023-00262-6>.

Additional file 1: Table S1. The Basic Physicochemical Properties of Soil and Biochar. **Table S2.** Topological Properties of the Co-occurrence Network for the Microbial Communities. **Fig S1.** Principal Coordinate Analysis (PCoA) shows how different biochar treatments affect *phoD*- (a) and *phoC*-harboring (b) microbial communities. Different biochar additions are shown in different colors, while soils A and B are represented by different symbols. Abbreviations: CK, no biochar addition; SBL, 0.5% straw biochar addition; SBH, 1% straw biochar addition; MBL, 0.5% manure biochar addition; MBH, 1% manure biochar addition. **Fig S2.** FTIR spectrum of straw biochar and manure biochar.

Acknowledgements

We are thankful to Zhejiang University, Griffith University, and Chinese Academy of Sciences for their financial support and research facilities. We also appreciate constructive comments from the editors and reviewers.

Author contributions

XW: roles/writing—original draft, investigation, methodology, formal analysis. HG: writing—review and editing. YF: writing—review and editing. CL: writing—review and editing. KME: visualization, writing—review and editing. ZW: Writing—review and editing. XL: supervision, funding acquisition, Writing—review and editing.

Funding

The study was financially supported by the National Natural Science Foundation of China (42277005; 22076163), the Key Research and Development Project of Science and Technology Department of Zhejiang Province (2023C02016; 2023C02019), and Bingtuan Science and Technology Program (2021DB019).

Availability of data and materials

The datasets used or analyzed during the current study are available from the corresponding author on reasonable request.

Declarations**Competing interests**

The author declare that they have no known competing financial interests or personal relationships that could have appeared to influence the work reported in this paper.

Author details

¹Key Laboratory of Watershed Non-point Source Pollution Control and Water Eco-security of Ministry of Water Resources, College of Environmental and Resource Sciences, Zhejiang University, Hangzhou 310058, China. ²College of Agriculture and Biotechnology, Zhejiang University, Hangzhou 310058, China. ³Australian Rivers Institute, School of Environment and Science, Griffith University, Nathan Campus, Brisbane, QLD 4111, Australia. ⁴Key Laboratory of Mollisols Agroecology, Northeast Institute of Geography and Agroecology, Chinese Academy of Sciences, Harbin 150081, China.

Received: 29 April 2023 Revised: 4 September 2023 Accepted: 9 September 2023

Published online: 21 September 2023

References

- Aanderud ZT, Saurey S, Ball BA, Wall DH, Barrett JE, Muscarella ME, Griffin NA, Virginia RA, Adams BJ (2018) Stoichiometric shifts in soil C:N: P promote bacterial taxa dominance, maintain biodiversity, and deconstruct community assemblages. *Front Microbiol.* <https://doi.org/10.3389/fmicb.2018.01401>
- Bello A, Han Y, Zhu H, Deng L, Yang W, Meng Q, Sun Y, Egbeagu UU, Sheng S, Wu X, Jiang X, Xu X (2020) Microbial community composition, co-occurrence network pattern and nitrogen transformation genera response to biochar addition in cattle manure-maize straw composting. *Sci Total Environ.* <https://doi.org/10.1016/j.scitotenv.2020.137759>
- Benjamini Y, Hochberg Y (1995) Controlling the false discovery rate: a practical and powerful approach to multiple testing. *J R Stat Soc: Ser B (Methodol)* 57:289–300. <https://doi.org/10.1111/j.2517-6161.1995.tb02031.x>
- Bergkemper F, Schöler A, Engel M, Lang F, Krüger J, Schloter M, Schulz S (2016) Phosphorus depletion in forest soils shapes bacterial communities towards phosphorus recycling systems. *Environ Microbiol* 18:1988–2000. <https://doi.org/10.1111/1462-2920.13188>
- Bi QF, Li KJ, Zheng BX, Liu XP, Li HZ, Jin BJ, Ding K, Yang XR, Lin XY, Zhu YG (2020) Partial replacement of inorganic phosphorus (P) by organic manure reshapes phosphate mobilizing bacterial community and promotes P bioavailability in a paddy soil. *Sci Total Environ.* <https://doi.org/10.1016/j.scitotenv.2019.134977>
- Blackwell MSA, Brookes PC, de la Fuente-Martinez N, Murray PJ, Snars KE, Williams JK, Haygarth PM (2009) Effects of soil drying and rate of re-wetting on concentrations and forms of phosphorus in leachate. *Biol Fertil Soils* 45:635–643. <https://doi.org/10.1007/s00374-009-0375-x>
- Bolln J, Faes J, Fritzsche A, Smolders E (2017) Colloidal-bound polyphosphates and organic phosphates are bioavailable: a nutrient solution study. *J Agric Food Chem* 65:6762–6770. <https://doi.org/10.1021/acs.jafc.7b01483>
- Bolyen E, Rideout JR, Dillon MR, Bokulich NA, Abnet CC, Al-Ghalith GA, Alexander H, Alm EJ, Arumugam M, Asnicar F, Bai Y, Bisanz JE, Bittinger K, Brejnrod A, Brislawn CJ, Brown CT, Callahan BJ, Caraballo-Rodríguez AM, Chase J, Cope EK, da Silva R, Diener C, Dorrestein PC, Douglas GM, Durall DM, Duvallet C, Edwardson CF, Ernst M, Estaki M, Fouquier J, Gauglitz JM, Gibbons SM, Gibson DL, Gonzalez A, Gorlick K, Guo J, Hillmann B, Holmes S, Holste H, Huttenhower C, Huttley GA, Janssen S, Jarmusch AK, Jiang L, Kaehler BD, bin Kang K, Keefe CR, Keim P, Kelley ST, Knights D, Koester I, Kosciorek T, Kreps J, Langille MGI, Lee J, Ley R, Liu YX, Löffler E, Lozupone C, Maher M, Marotz C, Martin BD, McDonald D, McIver LJ, Melnik AV, Metcalf JL, Morgan SC, Morton JT, Naimey AT, Navas-Molina JA, Nothias LF, Orchanian SB, Pearson T, Peoples SL, Petras D, Preuss ML, Pruesse E, Rasmussen LB, Rivers A, Robeson MS, Rosenthal P, Segata N, Shaffer M, Shiffer A, Sinha R, Song SJ, Spear JR, Swafford AD, Thompson LR, Torres PJ, Trinh P, Tripathi A, Turnbaugh PJ, Ul-Hasan S, van der Hooft JJJ, Vargas F, Vázquez-Baeza Y, Vogtmann E, von Hippel M, Walters W, Wan Y, Wang M, Warren J, Weber KC, Williamson, Willis AD, Xu ZZ, Zaneveld JR, Zhang Y, Zhu Q, Knight R, Caporaso JG. (2019) Reproducible, interactive, scalable and extensible microbiome data science using QIIME 2. *Nat Biotechnol.* <https://doi.org/10.1038/s41587-019-0209-9>
- Chen L, Jiang Y, Liang C, Luo Y, Xu Q, Han C, Zhao Q, Sun B (2019a) Correction to: competitive interaction with keystone taxa induced negative priming under biochar amendments. *Microbiome* 7:1–18. <https://doi.org/10.1186/s40168-019-0765-8>
- Chen X, Jiang N, Condrón LM, Dunfield KE, Chen Z, Wang J, Chen L (2019b) Impact of long-term phosphorus fertilizer inputs on bacterial phoD gene community in a maize field. *Sci Total Environ, Northeast China.* <https://doi.org/10.1016/j.scitotenv.2019.03.172>
- Chen H, Jarosch KA, Mészáros É, Frossard E, Zhao X, Oberson A (2021) Repeated drying and rewetting differently affect abiotic and biotic soil phosphorus (P) dynamics in a sandy soil: a 33P soil incubation study. *Soil Biol Biochem.* <https://doi.org/10.1016/j.soilbio.2020.108079>
- Chigineva NI, Aleksandrova Av, Tiunov Av (2009) The addition of labile carbon alters litter fungal communities and decreases litter decomposition rates. *Appl Soil Ecol* 42:264–270. <https://doi.org/10.1016/j.apsoil.2009.05.001>
- Eltohamy KM, Liu C, Khan S, Niyungeko C, Jin Y, Hosseini SH, Li F, Liang X (2021) An internet-based smart irrigation approach for limiting phosphorus release from organic fertilizer-amended paddy soil. *J Clean Prod* 293:126254. <https://doi.org/10.1016/j.jclepro.2021.126254>
- Feng W, Cui H, Zhu H, Shutes B, Yan B, Hou S (2023) Layered double hydroxides, an effective nanomaterial to remove phosphorus from wastewater: performance, mechanism, factors and reusability. *Sci Total Environ* 884:163757. <https://doi.org/10.1016/j.scitotenv.2023.163757>
- Fish JA, Chai B, Wang Q, Sun Y, Brown CT, Tiedje JM, Cole JR (2013) FunGene: the functional gene pipeline and repository. *Front Microbiol.* <https://doi.org/10.3389/fmicb.2013.00291>
- Fraser TD, Lynch DH, Gaiero J, Khosla K, Dunfield KE (2017) Quantification of bacterial non-specific acid (phoC) and alkaline (phoD) phosphatase genes in bulk and rhizosphere soil from organically managed soybean fields. *Appl Soil Ecol* 111:48–56. <https://doi.org/10.1016/j.apsoil.2016.11.013>
- Gaiero JR, Bent E, Fraser TD, Condrón LM, Dunfield KE (2018) Validating novel oligonucleotide primers targeting three classes of bacterial non-specific acid phosphatase genes in grassland soils. *Plant Soil* 427:39–51. <https://doi.org/10.1007/s11104-017-3338-2>
- Gao S, DeLuca TH (2018) Wood biochar impacts soil phosphorus dynamics and microbial communities in organically-managed croplands. *Soil Biol Biochem* 126:144–150. <https://doi.org/10.1016/j.soilbio.2018.09.002>
- Gao D, Bai E, Li M, Zhao C, Yu K, Hagedorn F (2020) Responses of soil nitrogen and phosphorus cycling to drying and rewetting cycles: a meta-analysis. *Soil Biol Biochem.* <https://doi.org/10.1016/j.soilbio.2020.107896>
- Gaskin JW, Steiner C, Harris K, Das KC, Bibens B (2008) Effect of low-temperature pyrolysis conditions on biochar for agriculture use. *Trans ASABE* 51:2061–2069
- Gu S, Gruau G, Malique F, Dupas R, Petitjean P, Gascuel-Oudoux C (2018) Drying/rewetting cycles stimulate release of colloidal-bound phosphorus in riparian soils. *Geoderma* 321:32–41. <https://doi.org/10.1016/j.geoderma.2018.01.015>
- Gu S, Gruau G, Dupas R, Jeanneau L (2020) Evidence of colloids as important phosphorus carriers in natural soil and stream waters in an agricultural catchment. *J Environ Qual* 49:921–932. <https://doi.org/10.1002/jeq2.20090>
- Han L, Qian L, Yan J, Chen M (2017) Effects of the biochar aromaticity and molecular structures of the chlorinated organic compounds on the adsorption characteristics. *Environ Sci and Pollut R* 24:5554–5565. <https://doi.org/10.1007/s11356-016-8303-8>
- Hens M, Merckx R (2001) Functional characterization of colloidal phosphorus species in the soil solution of sandy soils. *Environ Sci Technol* 35:493–500. <https://doi.org/10.1021/es0013576>
- Hens M, Merckx R (2002) The role of colloidal particles in the speciation and analysis of dissolved phosphorus. *Water Res* 36:1483–1492. [https://doi.org/10.1016/S0043-1354\(01\)00349-9](https://doi.org/10.1016/S0043-1354(01)00349-9)

- Heuck C, Weig A, Spohn M (2015) Soil microbial biomass C: N: P stoichiometry and microbial use of organic phosphorus. *Soil Biol Biochem* 85:119–129. <https://doi.org/10.1016/j.soilbio.2015.02.029>
- Huang Y, Dai Z, Lin J, Li D, Ye H, Dahlgren RA, Xu J (2021) Labile carbon facilitated phosphorus solubilization as regulated by bacterial and fungal communities in *Zea mays*. *Soil Biol Biochem* 163:108465. <https://doi.org/10.1016/j.soilbio.2021.108465>
- Islam MU, Jiang F, Guo Z, Peng X (2021) Does biochar application improve soil aggregation? A meta-analysis. *Soil Tillage Res* 209:104926. <https://doi.org/10.1016/j.still.2020.104926>
- Jacomy M, Venturini T, Heymann S, Bastian M (2014) ForceAtlas2, a continuous graph layout algorithm for handy network visualization designed for the Gephi software. *PLoS ONE*. <https://doi.org/10.1371/journal.pone.0098679>
- Jiang Z, Yan L, Wu J, Liu X, Zhang J, Zheng Y, Pei Y (2020) Low-temperature synthesis of carbonate-intercalated NiFe-layered double hydroxides for enhanced adsorption properties. *Appl Surf Sci*. <https://doi.org/10.1016/j.apsusc.2020.147281>
- Li F, Liang X, Li H, Jin Y, Jin J, He M, Klumpp E, Bol R (2020) Enhanced soil aggregate stability limits colloidal phosphorus loss potentials in agricultural systems. *Environ Sci Eur*. <https://doi.org/10.1186/s12302-020-0299-5>
- Li Y, Zhao Y, Cheng K, Yang F (2022) Effects of biochar on transport and retention of phosphorus in porous media: laboratory test and modeling. *Environ Pollut*. <https://doi.org/10.1016/j.envpol.2022.118788>
- Luo G, Sun B, Li L, Li M, Liu M, Zhu Y, Guo S, Ling N, Shen Q (2019) Understanding how long-term organic amendments increase soil phosphatase activities: insight into phod- and phoc-harboring functional microbial populations. *Soil Biol Biochem*. <https://doi.org/10.1016/j.soilbio.2019.107632>
- Ma L, Zhang J, Li Z, Xin X, Guo Z, Wang D, Li DC, Zhao B (2020) Long-term phosphorus deficiency decreased bacterial-fungal network complexity and efficiency across three soil types in China as revealed by network analysis. *Appl Soil Ecol*. <https://doi.org/10.1016/j.apsoil.2020.103506>
- Nannipieri P, Trasar-Cepeda C, Dick RP (2018) Soil enzyme activity: a brief history and biochemistry as a basis for appropriate interpretations and meta-analysis. *Biol Fertil Soils* 54:11–19. <https://doi.org/10.1007/s00374-017-1245-6>
- Novair SB, Hosseini HM, Etesami H, Razavipour T (2021) Impact of drying-rewetting cycles and organic amendments on phosphorus speciation of paddy soil. *Soil Res* 59:472–487. <https://doi.org/10.1071/SR20308>
- Pagel H, Ilg K, Siemens J, Kaupenjohann M (2008) Total phosphorus determination in colloid-containing soil solutions by enhanced persulfate digestion. *Soil Sci Soc Am J* 72:786–790. <https://doi.org/10.2136/sssaj2007.0178n>
- Palansooriya KN, Wong JTF, Hashimoto Y, Huang L, Rinklebe J, Chang SX, Bolan N, Wang H, Ok YS (2019) Response of microbial communities to biochar-amended soils: a critical review. *Biochar* 1:3–22. <https://doi.org/10.1007/s42773-019-00009-2>
- Powers SM, Bruulsema TW, Burt TP, Chan NI, Elser JJ, Haygarth PM, Howden NJK, Jarvie HP, Lyu Y, Peterson HM, Sharpley AN, Shen J, Worrall F, Zhang F (2016) Long-term accumulation and transport of anthropogenic phosphorus in three river basins. *Nat Geosci* 9:353–356. <https://doi.org/10.1038/ngeo2693>
- Ragot SA, Huguenin-Elie O, Kertesz MA, Frossard E, Bünemann EK (2016) Total and active microbial communities and phoD as affected by phosphate depletion and pH in soil. *Plant Soil* 408:15–30. <https://doi.org/10.1007/s11104-016-2902-5>
- Renella G, Landi L, Ascher J, Ceccherini MT, Pietramellara G, Nannipieri P (2006) Phosphomonoesterase production and persistence and composition of bacterial communities during plant material decomposition in soils with different pH values. *Soil Biol Biochem* 38:795–802. <https://doi.org/10.1016/j.soilbio.2005.07.005>
- Saffari N, Hajabbasi MA, Shirani H, Mosaddeghi MR, Mamedov AI (2020) Biochar type and pyrolysis temperature effects on soil quality indicators and structural stability. *J Environ Manage* 261:110190. <https://doi.org/10.1016/j.jenvman.2020.110190>
- Sakurai M, Wasaki J, Tomizawa Y, Shinano T, Osaki M (2008) Analysis of bacterial communities on alkaline phosphatase genes in soil supplied with organic matter. *Soil Sci Plant Nutr* 54:62–71. <https://doi.org/10.1111/j.1747-0765.2007.00210.x>
- Schindler DW, Carpenter SR, Chapra SC, Hecky RE, Orihel DM (2016) Reducing phosphorus to curb lake eutrophication is a success. *Environ Sci Technol* 50:8923–8929. <https://doi.org/10.1021/acs.est.6b02204>
- Spohn M, Kuzyakov Y (2013) Phosphorus mineralization can be driven by microbial need for carbon. *Soil Biol Biochem* 61:69–75. <https://doi.org/10.1016/j.soilbio.2013.02.013>
- Sun D, Bi Q, Xu H, Li K, Liu X, Zhu J, Zhang Q, Jin C, Lu L, Lin X (2017) Degree of short-term drying before rewetting regulates the bicarbonate-extractable and enzymatically hydrolyzable soil phosphorus fractions. *Geoderma* 305:136–143. <https://doi.org/10.1016/j.geoderma.2017.05.040>
- Tabatabai MA, Bremner JM (1969) Use of p-nitrophenyl phosphate for assay of soil phosphatase activity. *Soil Biol Biochem*. Pzrigamon Press
- Tian J, Kuang X, Tang M, Chen X, Huang F, Cai Y, Cai K (2021) Biochar application under low phosphorus input promotes soil organic phosphorus mineralization by shifting bacterial phoD gene community composition. *Sci Total Environ*. <https://doi.org/10.1016/j.scitotenv.2021.146556>
- Turner BL, Driessen JP, Haygarth PM, McKelvie ID (2003) Potential contribution of lysed bacterial cells to phosphorus solubilisation in two rewetted Australian pasture soils. *Soil Biol Biochem* 35:187–189. [https://doi.org/10.1016/S0038-0717\(02\)00244-4](https://doi.org/10.1016/S0038-0717(02)00244-4)
- van Dinh M, Guhr A, Spohn M, Matzner E (2017) Release of phosphorus from soil bacterial and fungal biomass following drying/rewetting. *Soil Biol Biochem* 110:1–7. <https://doi.org/10.1016/j.soilbio.2017.02.014>
- Walker TW, Adams AFR (1959) Studies on soil organic matter: I. Influence of phosphorus content of parent materials on accumulations of carbon, nitrogen, sulfur, and organic phosphorus in grassland soil. *Soil Sci*. <https://doi.org/10.1097/00010694-195901000-00001>
- Wang Q, Wang C, Yu WW, Turak A, Chen D, Huang Y, Ao J, Jiang Y, Huang Z (2018) Effects of nitrogen and phosphorus inputs on soil bacterial abundance, diversity, and community composition in Chinese fir plantations. *Front Microbiol*. <https://doi.org/10.3389/fmicb.2018.01543>
- Wang C, Guo J, Zhang W, Jiang Y, Fang F, He W, Jia B, Dang C (2021a) Drying-rewetting changes soil phosphorus status and enzymatically hydrolysable organic phosphorus fractions in the water-level fluctuation zone of three Gorges reservoir. *Catena (Amst)*. <https://doi.org/10.1016/j.catena.2021.105416>
- Wang Q, Xu L, Guo D, Wang G, Song X, Ma Y (2021b) The continuous application of biochar in field: effects on P fraction, Chemosphere, P sorption and release. <https://doi.org/10.1016/j.chemosphere.2020.128084>
- Wang Z, Chen L, Liu C, Jin Y, Li F, Khan X (2021c) Reduced colloidal phosphorus loss potential and enhanced phosphorus availability by manure-derived biochar addition to paddy soils. *Geoderma* 402:115348. <https://doi.org/10.1016/j.geoderma.2021.115348>
- Wang X, Eltohamy KM, Liu C, Li F, Fang Y, Kawasaki A, Liang X (2023) Biochar reduces colloidal phosphorus in soil aggregates: the role of microbial communities. *J Environ Manage* 326:116745. <https://doi.org/10.1016/j.jenvman.2022.116745>
- Wei X, Hu Y, Razavi BS, Zhou J, Shen J, Nannipieri P, Wu J, Ge T (2019) Rare taxa of alkaline phosphomonoesterase-harboring microorganisms mediate soil phosphorus mineralization. *Soil Biol Biochem* 131:62–70. <https://doi.org/10.1016/j.soilbio.2018.12.025>
- Xu G, Sun JN, Shao HB, Chang SX (2014) Biochar had effects on phosphorus sorption and desorption in three soils with differing acidity. *Ecol Eng* 62:54–60. <https://doi.org/10.1016/j.ecoleng.2013.10.027>
- Yan T, Xue J, Zhou Z, Wu Y (2021) Biochar-based fertilizer amendments improve the soil microbial community structure in a karst mountainous area. *Sci Total Environ*. <https://doi.org/10.1016/j.scitotenv.2021.148757>
- Yan X, Qian J, Wang S, Zhang X, Zhang Y, Pan B (2022) Selective removal of organic phosphonates via coupling hyper-cross-linked resin with nanoconfined hydrated oxides. *Chem Eng J*. <https://doi.org/10.1016/j.cej.2021.132620>
- Yang C, Lu S (2022) Straw and straw biochar differently affect phosphorus availability, enzyme activity and microbial functional genes in an Ultisol. *Sci Total Environ*. <https://doi.org/10.1016/j.scitotenv.2021.150325>
- Yang F, Zhang S, Sun Y, Tsang DCW, Cheng K, Ok YS (2019) Assembling biochar with various layered double hydroxides for enhancement of phosphorus recovery. *J Hazard Mater* 365:665–673. <https://doi.org/10.1016/j.jhazmat.2018.11.047>
- Yang W, Shang J, Li B, Flury M (2020) Surface and colloid properties of biochar and implications for transport in porous media. *Crit Rev Environ Sci Technol* 50:2484–2522. <https://doi.org/10.1080/10643389.2019.1699381>
- Yang B, Lin H, Bartlett SL, Houghton EM, Robertson DM, Guo L (2021a) Partitioning and transformation of organic and inorganic phosphorus among

- dissolved, colloidal and particulate phases in a hypereutrophic freshwater estuary. *Water Res.* <https://doi.org/10.1016/j.watres.2021.117025>
- Yang L, Wu Y, Wang Y, An W, Jin J, Sun K, Wang X (2021b) Effects of biochar addition on the abundance, speciation, availability, and leaching loss of soil phosphorus. *Sci Total Environ.* <https://doi.org/10.1016/j.scitotenv.2020.143657>
- Yang L, Han W, Zhao W, Gu C, Xu Z, Jiang X (2023) Mono-/multiadsorption of chlorobenzene compounds on biochar: influence of the properties of the chlorobenzene molecules and biochar. *J Soils Sediments* 23:2120–2135. <https://doi.org/10.1007/s11368-023-03478-y>
- Zhu W, Zhao X, Wang SQ, Wang Y (2019) Inter-annual variation in P speciation and availability in the drought-rewetting cycle in paddy soils. *Agric Ecosyst Environ.* <https://doi.org/10.1016/j.agee.2019.106652>

Submit your manuscript to a SpringerOpen[®] journal and benefit from:

- ▶ Convenient online submission
- ▶ Rigorous peer review
- ▶ Open access: articles freely available online
- ▶ High visibility within the field
- ▶ Retaining the copyright to your article

Submit your next manuscript at ▶ [springeropen.com](https://www.springeropen.com)
